

Rate Constants for the $\text{CH}_4 + \text{H} \rightarrow \text{CH}_3 + \text{H}_2$ Reaction Calculated with a Generalized Reduced-Dimensionality Method[†]

Juliana Palma and Julián Echave

Centro de Estudios e Investigaciones, Universidad Nacional de Quilmes, Sáenz Peña 180, B1876BXD Bernal, Argentina

David C. Clary*

Department of Chemistry, University College London, 20 Gordon Street, London, WC1H 0AJ, U.K.

Received: October 31, 2001; In Final Form: January 4, 2002

We present calculations of rate constants for the $\text{CH}_4 + \text{H} \rightarrow \text{CH}_3 + \text{H}_2$ reaction. Calculations were performed using a reduced-dimensionality model with four degrees of freedom and two different methods to convert reduced-dimensionality reaction probabilities into rate constants. In one method, an energy shifting correction is performed using the vibrational frequencies of the reaction complex at the classical transition state. In the other method, the correction is done using the frequencies at a vibrationally adiabatic transition state. These approximate rate constants are compared against the full-dimensional values recently presented by Manthe et al. to determine which of these approaches is the more appropriate.

I. Introduction

Several reduced-dimensionality (RD) quantum scattering models have been developed recently to study hydrogen abstraction reactions from methane.^{1–9} These models allow studying the state-to-state dynamics of these reactions over selected degrees of freedom. Thermal rate constants can also be estimated by applying an energy shifting correction^{10,11} that takes into account the effect of the degrees of freedom not explicitly considered by the models.

The energy shifting correction is normally performed using the vibrational energies of the reaction complex at the classical transition state (CTS), that is, at the maximum of the potential energy along the minimum energy path.¹⁰ Recently, we proposed a new procedure in which the correction is done using the energies at a generalized transition state (GTS).¹² The GTS was defined as the barrier of the ground-state vibrationally adiabatic potential energy surface.

We applied the GTS method to the $\text{O}(^3\text{P}) + \text{CH}_4 \rightarrow \text{OH} + \text{CH}_3$ reaction, and we found that the RD-GTS rate constants agreed much better with experimental results than the RD-CTS ones. This result was very encouraging, but it does not give a definite test of the GTS method as the results of dynamical calculations strongly depend on the quality of the potential energy surface (PES). A more rigorous test would involve the comparison between RD-GTS and full-dimensional rate constants obtained with the same PES. So far, no exact calculations have been performed for the $\text{O}(^3\text{P}) + \text{CH}_4 \rightarrow \text{OH} + \text{CH}_3$ reaction, and therefore, that rigorous test could not be done.

Recently, Manthe et al. calculated rate constants based on full-dimensional $J = 0$ probabilities^{13–15} for

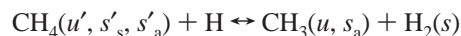


using the PES developed by Jordan and Gilbert.¹⁶ These results give us the opportunity to perform a more rigorous test of the GTS method. The findings of such a test are presented in this paper.

The rest of the paper is organized as follows. In section II, we briefly describe the theory used to get RD reaction probabilities and rate constants. Numerical details are given in section III. The comparison between full-D and RD rate constants is presented in section IV along with a discussion of previous RD studies of reaction 1. Conclusions are given in section V.

II. Theory

Reduced-dimensionality calculations were performed with a four degrees of freedom model that has been described in detail elsewhere.⁵ Therefore, we present here just a brief discussion of the method. Figure 1 shows the degrees of freedom explicitly considered by the model. The reaction considered is



with u and s being the quantum numbers for the umbrella and stretching vibrations, respectively, with subscripts s and a standing for symmetric and asymmetric, respectively.

The Hamiltonian used in the reduced-dimensionality calculations was

$$\hat{H} = -\frac{\hbar^2}{2\mu} \frac{\partial^2}{\partial \rho^2} - \frac{\hbar^2}{2\mu \rho^2} \frac{\partial^2}{\partial \delta^2} + \frac{3\hbar^2}{8\mu \rho^2} + \frac{\hat{J}^2}{2\mu \rho^2} + \hat{K}_{\text{CH}_3}^{\text{vib}} \quad (2)$$

where \hat{J} is the total angular momentum, $\mu = (m_{\text{H}}^2 m_{\text{CH}_3} / m_{\text{TOT}})^{1/2}$, $m_{\text{TOT}} = 2m_{\text{H}} + m_{\text{CH}_3}$ and

$$\hat{K}_{\text{CH}_3}^{\text{vib}} = -\frac{\hbar^2}{2\mu_x} \frac{\partial^2}{\partial x^2} - \frac{\hbar^2}{2\mu_s} \frac{\partial^2}{\partial s^2}$$

with $\mu_x = 3m_{\text{H}}$ and $\mu_s = 3m_{\text{H}}m_{\text{C}}/(m_{\text{C}} + 3m_{\text{H}})$. The hyperspheri-

[†] Part of the special issue "Donald Setser Festschrift".

* To whom correspondence should be addressed. E-mail: d.c.clary@ucl.ac.uk.

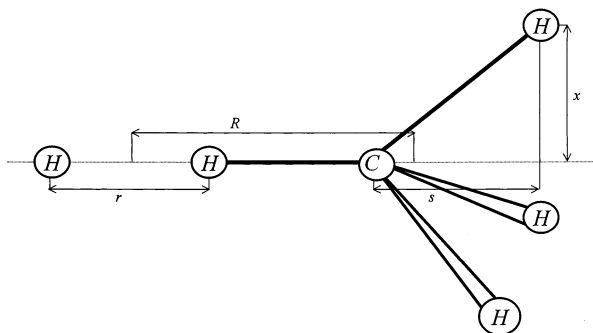


Figure 1. Variables for the reduced-dimensionality model.

cal variables ρ and δ were defined in the usual way from the Jacobi coordinates R and r shown in Figure 1. The corresponding volume element is $d\tau = d\rho d\delta dx ds$.

The close coupling equations for the Hamiltonian (eq 2) with $J = 0$ were propagated using the R -matrix method.¹⁷ The whole range of the hyperradius, $\rho_{\min} \leq \rho \leq \rho_{\max}$ was divided into N_ρ sectors, and within each sector, the wave function was expanded as

$$\Psi_{n'} = \sum_n^{N_{cc}} f_{nn'}(\rho; \rho_i) \psi_n(\delta, x, s; \rho_i)$$

Here ρ_i is the value of ρ at the center of the i th sector and n' (u' , s'_s , s'_a) indicates the initial quantum state. The hyperspherical adiabats were expanded as

$$\psi_n(\delta, x, s; \rho_i) = \sum_{n_\delta}^{N_\delta^{\text{PO}}} \sum_{n_x}^{N_x^{\text{PO}}} \sum_{n_s}^{N_s^{\text{PO}}} c_{n_\delta n_x n_s}^n \psi_{n_\delta}^{\text{PO}}(\delta; \rho_i) \psi_{n_x}^{\text{PO}}(x; \rho_i) \psi_{n_s}^{\text{PO}}(s; \rho_i)$$

where the $\psi_{n_\xi}^{\text{PO}}(\xi; \rho_i)$ functions are potential optimized discrete variable representation basis functions¹⁸ for the variables $\xi = \delta, x, \text{ or } s$. The way in which these functions were obtained has been explained elsewhere.^{5,8}

At large values of ρ , the hyperspherical adiabats become the quantum states of either H + CH₄(u', s'_s, s'_a) for large values of δ or CH₃(u, s_s) + H₂(s) for $\delta \approx 0$. Thus, we used the expectation value $\langle \psi_n(\delta, x, s; \rho_i) | \delta | \psi_{n'}(\delta, x, s; \rho_i) \rangle$ to classify the asymptotic states. We applied approximate boundary conditions at each sector between ρ_a and ρ_b to obtain the S matrix elements $S_{n'n,i}^-(E)$, at total energy, E . Reduced-dimensionality state-to-state reaction probabilities, $P_{n'n}(E)$, were obtained by averaging $|S_{n'n,i}^-|^2$ over sectors and cumulative probabilities, $P_{\text{cum}}(E)$, were obtained by summing $P_{n'n}(E)$ over n' and n .

Reduced-dimensionality rate constants were calculated using the J -shifting and energy-shifting approximation^{10,11} from

$$k(T) = \frac{Q^\ddagger(T)}{2\pi\hbar Q_{\text{CH}_4}(T) Q_{\text{rel}}(T)} \int_0^\infty dE P_{\text{cum}}(E) e^{-E/(k_B T)}$$

Here Q^\ddagger is the partition function for the transition state, Q_{CH_4} is the partition function for reactant CH₄, and Q_{rel} is the partition function for the relative motion between H and CH₄. The partition functions Q and Q_{CH_4} contain a rotational and a vibrational contribution. The vibrational contribution to Q involves only the vibrational modes of the transition state not considered by the reduced-dimensionality model. In both cases, the vibrational partition functions were calculated using the harmonic frequencies.

TABLE 1: Correlation between Full-D and RD Normal Modes of Reactants and Products

	full-D	RD	frequency, cm ⁻¹
CH ₄	$\nu_1(a_1)$	s'_s	2887
	$\nu_2(e)$		1502
	$\nu_3(t_2)$	s'_a	3053
	$\nu_4(t_2)$	u'	1340
CH ₃	$\nu_1(a'_1)$	s_s	3010
	$\nu_2(a'_2)$	u	580
	$\nu_3(e')$		3180
	$\nu_4(e')$		1384
H ₂	$\nu(\sigma_g)$	s	4407

III. Numerical Details

For the present calculations, we used the PES originally developed by Jordan and Gilbert¹⁶ and then modified by Huarte-Larrañaga and Manthe at the time of doing their full-D calculations.¹⁵ The modification renders a surface that is symmetric with respect to the exchange of the H atoms of CH₄. On this surface, reaction 1 has a transition state with symmetry C_{3v} which is 0.474 eV above the potential energy of the reactants at equilibrium.

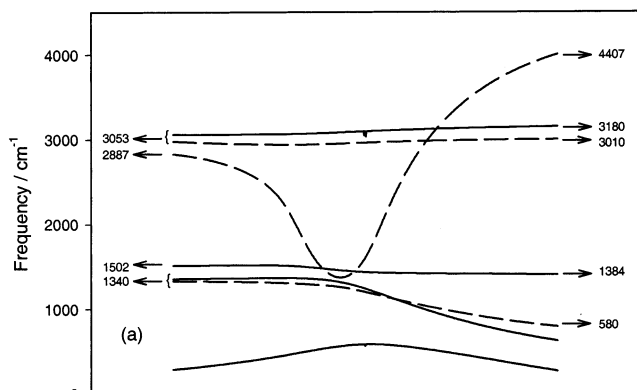
Table 1 presents the correlation between the vibrational modes considered by the model used for the present calculations and those corresponding to the full-dimensional system, along with their harmonic frequencies. It is worth noting that the harmonic frequencies of reactants, products, and transition state for the RD model are exactly the same as their full-dimensional counterparts.⁵ This implies that the model does not distort or mix the normal modes that it considers explicitly. Because of this, there are no ambiguities at the time of identifying the normal modes of reactants and transition state not considered in the scattering calculations. This is an important difference between our model and some other models used to study reaction 1, as we will see later.

We followed the methodology developed by Truhlar and co-workers¹⁹ to determine the energies of the normal modes perpendicular to the reaction coordinate s , defined as the signed distance from the saddle point along the minimum energy path (MEP). The MEP is determined starting from the saddle point and going downhill to reactants and products. The energy-gradient vector and the force constant matrix are evaluated in Cartesian coordinates at a set of selected nonstationary points along the MEP and then transformed into an internal coordinate representation. Finally, the force matrix is projected to remove the reaction path components and vibrational frequencies are obtained using the Wilson GF-matrix method.²⁰ With this information, the ground-state vibrationally adiabatic potential energy curve was calculated as

$$V_g(s) = V_{\text{MEP}}(s) + \sum_k \epsilon_k^{n_k=0}(s)$$

where $V_{\text{MEP}}(s)$ is the value of the potential energy along the minimum energy path and $\epsilon_k^{n_k=0}(s)$ is the energy of the adiabatic mode k , for vibrational quantum number $n_k = 0$. The position of the generalized transition state was defined as the maximum of the $V_g(s)$ curve. Figure 2a shows the variation of the harmonic frequencies along the reaction coordinate, while Figure 2b shows the potential, zero-point energy, and ground-state vibrationally adiabatic potential energy curves. As can be seen there, the generalized transition state is on the reactant side. The values of the harmonic frequencies at the classical and generalized transition state are given in Table 2.

The values of the parameters used in the close coupling calculations are given in Table 3. Note that not all of the



parameters appearing in this table were defined in Section II because we only presented there a brief review of the methodology. A complete explanation of all of the parameters appearing in Table 3 can be found in ref 5.

IV. Results and Discussion

Reduced-dimensionality (RD-CTS and RD-GTS) rate constants are shown in Figure 3, along with the full-dimensional values of ref 13, for temperatures between 200 and 500 K. We can see that both RD-CTS and RD-GTS rate constants underestimate the full-dimensional values, although the results do become very close at 500 K. The differences are probably due to limitations of the RD model that we used to get the cumulative probabilities. According to the full-dimensional study of Huarte-Larrañaga and Manthe,¹⁴ the vibrational modes mainly participating in the reactive event are those with frequencies of 1093i, 1602, and 1205 cm^{-1} at the transition state. As can be seen in Table 2, our RD model does explicitly consider these modes. However, they also found that the doubly degenerate bending modes with frequencies of 587 and 1245 cm^{-1} had a nonnegligible role in the dynamics¹⁴ These modes are frozen in our model. The lack of flexibility in these modes that can couple to the movement along the reaction coordinate probably explains the fact that our RD rate constants underestimate the full-dimensional values. However, despite the limitations of the RD model, Figure 3 shows that RD-GTS rate constants represent a significant improvement over the standard RD-CTS ones. The ratio between full-D and RD-CTS rate constants is 17 at 200 K and 5 at 500 K, while for the RD-GTS rate constants the corresponding values are 5 and 1.2, respectively. This finding reinforces the idea that the use of a generalized transition state is more appropriate than the classical transition state for reduced-dimensionality calculations.

Other RD models have been applied to reaction 1. Takayanagi⁴ used a three-dimensional model, which approximately considers the modes with frequencies of 1093i, 1602, and 1205 cm^{-1} at the transition state. However, because his model does not consider the bending frequencies of 587 and 1245 cm^{-1} mentioned above, his rate constants also underestimate the full-dimensional values. Later, Yu and Nyman performed calculations with a four-dimensional model.² Their model approximately considers the modes with frequencies of 1093i, 1602, and 1205 cm^{-1} at the transition state, plus a bending mode that corresponds to the rocking movement of CH_3 with respect to the C–H bond being broken. With this model, they obtained rate constants in good agreement with the full-dimensional values, as was noted in ref 13. However, that good agreement might be fortuitous and could be due to the cancellation of two different errors. First, Yu and Nyman considered that the RD CH_4 molecule had a bending frequency of 2792 cm^{-1} , when the correct harmonic frequency is about one half of that value.⁹